Spatial Buffering of Light-Evoked Potassium Increases by Retinal Müller (Glial) Cells

CHESTER J. KARWOSKI, HONG-KAI LU, ERIC A. NEWMAN*

Activity-dependent variations in extracellular potassium concentration in the central nervous system may be regulated, in part, by potassium spatial buffering currents in glial cells. The role of spatial buffering in the retina was assessed by measuring light-evoked potassium changes in amphibian eyecups. The amplitude of potassium increases in the vitreous humor was reduced to ~10 percent by 50 micromolar barium, while potassium increases in the inner plexiform layer were largely unchanged. The decrease in the vitreal potassium response was accurately simulated with a numerical model of potassium current flow through Müller cells, the principal glial cells of the retina. Barium also substantially increased the input resistance of Müller cells and blocked the Müller cell–generated M-wave, indicating that barium blocks the potassium channels of Müller cells. Thus, after a light-evoked potassium increase within the retina, there is a substantial transfer of potassium from the retina to the vitreous humor by potassium current flow through Müller cells.

ORKAND, NICHOLLS, AND KUFFLER (*1*) proposed that the extracellular potassium concentration ($[K^+]_o$) in the brain is regulated, in part, by K^+ spatial buffering by glial cells. They suggested that an increase in $[K^+]_o$ generated by neuronal activity results in an influx of K^+ into glial cells, which are almost exclusively permeable to K^+ (*2*). This K^+ influx leads to cell depolarization and results in an efflux of an equal amount of K^+ from other cell regions. This cellular K^+ current transfers K^+ from regions where $[K^+]_o$ is high to regions where $[K^+]_o$ is lower. Although this theory has received support (*3, 4*), a direct demonstration of spatial buffering by glial cells in a normal, in situ preparation has been lacking. Large spatial buffering currents have been predicted to occur in the retina, where the Müller (glial) cell is well suited to transfer K^+ from the retina to the vitreous humor (*5, 6*). We have now tested for K^+ spatial buffering by monitoring light-evoked $[K^+]_o$ changes in the amphibian retina.

Changes in $[K^+]_o$ were measured with double-barreled K^+-selective microelectrodes containing Corning resin 477317 or a valinomycin-based liquid membrane, Fluka 60031. Recordings were made from frog and mudpuppy eyecups stimulated by flashes of white light (either diffuse light or a small spot). Eyecups were superfused with an amphibian Ringer's solution (*7*). The location of the K^+-selective electrode within the retina was determined by such criteria as electrode depth, the intraretinal electroretinogram (ERG), and resistance landmarks (*8*).

A characteristic series of light-evoked variations in $[K^+]_o$ occurs when the retina is stimulated with a light flash (Fig. 1A). In the inner plexiform layer (IPL) an increase in $[K^+]_o$ is seen at both the "ON" and "OFF" of the stimulus. This $[K^+]_o$ increase decays slowly over many seconds. As the electrode is withdrawn toward the retinal surface, this $[K^+]_o$ increase becomes smaller and decays more slowly. In the vitreous humor (20 μm above the retinal surface) the $[K^+]_o$ increase is significantly attenuated and decays very slowly (Fig. 1A).

When Ba^{2+} is added to the superfusate (Fig. 1B), the $[K^+]_o$ response in the IPL is largely unchanged in amplitude but decays somewhat slower. Similar changes occurred in the ganglion cell layer. However, a large Ba^{2+}-induced change occurs in the vitreous humor, where the $[K^+]_o$ ON response is decreased to 22% of its control amplitude (in the example shown) and has an extremely slow time course. Similar Ba^{2+}-induced changes in $[K^+]_o$ responses were recorded in experiments in both frog and mudpuppy eyecups. The vitreal $[K^+]_o$ response was reduced by Ba^{2+} to an average of 11% of the control value in frogs and 8% in salamanders (Table 1).

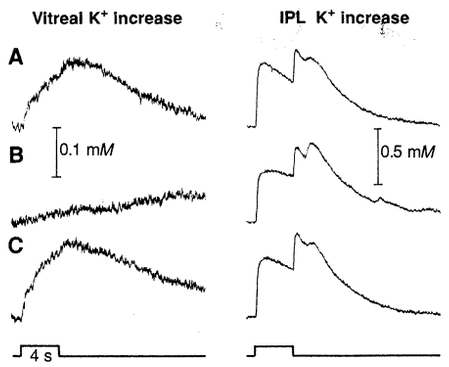

Fig. 1. Light-evoked $[K^+]_o$ changes in the vitreous humor and in the IPL (**A**) before, (**B**) approximately 5 min after Ba^{2+} application (50 μ*M*), and (**C**) approximately 1 hour after washout of a frog eyecup. The secondary peak in the IPL at light off is the delayed off response (*20*). Light stimulus (diffuse illumination; intensity, 3.2 lux) is indicated at the bottom. Here and in Fig. 2 the ordinate represents the linear K^+ concentration. Resting $[K^+]_o$ in the IPL, 2.7 m*M*.

Although Ba^{2+} treatment leads to only small changes in the light-evoked $[K^+]_o$ responses in the IPL, it causes a dramatic decrease in the $[K^+]_o$ response in the vitreous humor. This difference can be explained by hypothesizing that a large fraction of the vitreal $[K^+]_o$ increase comes from a K^+ spatial buffering current flowing through Müller cells, rather than from diffusion of K^+ through extracellular space. Ba^{2+} application would attenuate the vitreal $[K^+]_o$ increase by blocking Müller cell K^+ channels and thus interrupting the K^+ current.

The validity of this hypothesis is based on three assumptions. (i) Ba^{2+} does not greatly interfere with the diffusion of K^+ through extracellular space. This idea is supported by resistance measurements (*4*) that indicate that there are no significant changes in extracellular volume fraction or tortuosity (the effective length along which K^+ must diffuse) after Ba^{2+} application. (ii) Ba^{2+} does not act by blocking an active uptake process that transports K^+ to the vitreous humor. This is likely because Ba^{2+} blocks active K^+ uptake in glial cells only in concentrations higher than those that were used in our experiments (*9*) and because a ouabain-induced block of K^+ transport has little effect on current-evoked K^+ fluxes through Müller cells (*4*). (iii) Ba^{2+} blocks K^+ channels in Müller cells. Although Ba^{2+} is known to block K^+ channels in neurons (*10*) and in some glial cells (*11*), the situation in retinal cells is unclear because preliminary reports suggested that Ba^{2+} does not block K^+ channels in Müller cells in situ (*12*).

We assessed the effect of Ba^{2+} on Müller cells in situ by measuring cell input resistance before and after Ba^{2+} application. Intracellular recordings were made from retinal slices of the tiger salamander (*6*). Cells were penetrated in the soma, and input resistance was measured with depolarizing current pulses.

Müller cell input resistance was 10.9 ± 2.3 megohms (mean ± SEM, $n = 17$) in control Ringer's solution, close to the value of 9.7 megohms measured in isolated sala-

C. J. Karwoski and H.-K. Lu, Vision Research Laboratory, Department of Psychology, University of Georgia, Athens, GA 30602.
E. A. Newman, Eye Research Institute and Department of Ophthalmology, Harvard Medical School, Boston, MA 02114.

*To whom correspondence should be addressed at the Eye Research Institute, 20 Staniford Street, Boston, MA 02114.

mander Müller cells (*13*). Cell resistance rose to 50.4 ± 8.1 megohms in 50 μM Ba^{2+}; that is, conductance decreased to 22% of the control value (Table 1). Müller cells are almost exclusively permeable to K^+ (*6, 14*). Thus, these results demonstrate that Ba^{2+} blocks most K^+ channels of Müller cells in situ.

We obtained additional evidence that Ba^{2+} blocks most of the Müller cell K^+ conductance by monitoring the intraretinal (local) ERG. Within the IPL the local ERG consists of a fast upward deflection, the proximal negative response (PNR), followed by a slower potential, the M-wave (*15*) (Fig. 2A, field potential). Simultaneous $[K^+]_o$ recordings (Fig. 2A, IPL K^+ increase) show that the time course of the $[K^+]_o$ increase parallels that of the M-wave. After Ba^{2+} application (Fig. 2B), the M-wave is almost abolished while the PNR remains nearly unchanged. In this example, the $[K^+]_o$ increase is augmented slightly after Ba^{2+} application. Similar results were obtained from frog and mudpuppy (Table 1).

Both the PNR and the IPL $[K^+]_o$ increase are indicators of neural activity in the proximal retina (*15*). Thus, these results confirm that micromolar Ba^{2+} does not severely depress neuronal activity. However, the M-wave, which is believed to be generated by an influx of K^+ into Müller cells (*15, 16*), is severely depressed by Ba^{2+}. Thus, this experiment supports the supposition that Ba^{2+} blocks most Müller cell K^+ channels in situ while not seriously compromising neuronal activity.

Our results suggest that after an increase in retinal $[K^+]_o$ there is substantial K^+ current flow through Müller cells from the retina to the vitreous humor. We tested this hypothesis with one additional approach: the modeling of K^+ dynamics in the retina.

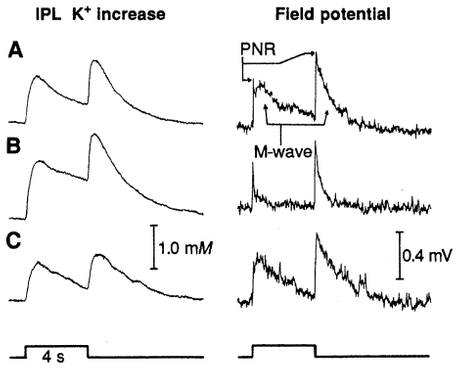

Fig. 2. The $[K^+]_o$ response and the intraretinal ERG (negative upward) recorded simultaneously in the IPL of frog (**A**) before, (**B**) approximately 5 min after Ba^{2+} application (50 μM), and (**C**) approximately 1 hour after washout. The PNR and the increase in $[K^+]_o$ were largely unaffected by Ba^{2+}, while the M-wave was greatly reduced. Stimulus, 0.3-mm spot; intensity, 3.2 lux.

We asked whether our experimental observation of the dominance of spatial buffering over diffusion in transporting K^+ to the vitreous humor is reasonable, given our knowledge of Müller cell conductance and retinal tissue geometry. We utilized the numerical model of Odette and Newman (*17*), with values of tissue parameters obtained from previously published results (*18*). Only the K^+ source and sink in the model were adjusted to produce a $[K^+]_o$ response in the IPL matching that recorded experimentally. We then simulated Ba^{2+} in the model by setting the Müller cell conductance equal to zero (a simplifying assumption) and by reducing the amplitude of the K^+ source and sink to 79% of the control value (so that simulated and experimental IPL responses in Ba^{2+} had equal amplitudes).

When we simulated the experiment in Fig. 1 (frog eyecup, diffuse illumination),

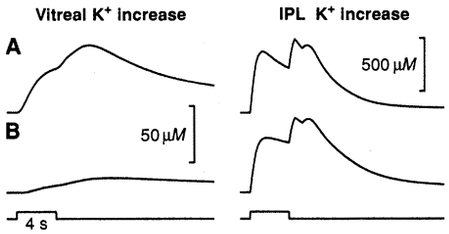

Fig. 3. Computer simulation of the experiment in Fig. 1, A and B. Simulated Ba^{2+} in the model (i) substantially reduced and slowed the $[K^+]_o$ increase in the vitreous and (ii) slowed the decay of the $[K^+]_o$ response in the IPL (*18*).

we obtained a good match with experimental results for both control and Ba^{2+} conditions (Fig. 3) (*19*). The simulation of Ba^{2+} resulted in a reduction of the vitreal $[K^+]_o$ response to 15% of its control amplitude, close to the 11% value obtained experimentally. In addition, the change in the time course of the simulated vitreal response was similar to that seen experimentally. The time to peak of the simulated vitreal response increased from 7.2 to 9.6 s with Ba^{2+}; corresponding times for the experimental responses averaged 5.9 and 9.8 s. In the IPL, the Ba^{2+}-induced changes in the time course of simulated and experimental $[K^+]_o$ responses were also similar. In both cases decay of the responses (both ON and OFF components) was slowed. The agreement between simulated and experimental responses lends further support to the hypothesis that K^+ spatial buffering current through Müller cells is important in transferring K^+ from the retina to the vitreous humor.

Our results provide evidence that a large fraction of the light-evoked $[K^+]_o$ increase in the vitreous humor is generated by K^+

Table 1. Amplitudes (mean ± SEM) of light-evoked $[K^+]_o$ increases and intraretinal ERGs from frog (*Rana pipiens*) and salamander (*Necturus maculosus*) eyecups and Müller cell conductance values from salamander (*Ambystoma tigrinum*) retinal slices. For frog, Ba^{2+} concentrations ranging from 40 to 100 μM were used in different experiments; for salamander, 50 μM Ba^{2+} was used in all experiments. For the computer simulation, $[K^+]_o$ amplitudes in the IPL were matched to the mean of the experimental results. Percentages indicate amplitude of response in Ba^{2+} relative to control amplitude.

Condition	Diffuse illumination				Spot, 0.3 mm			Müller cell conductance (nS)
	IPL K^+ increase (μM)	Simulation	Vitreal K^+ increase (μM)	Simulation	IPL K^+ increase (μM)	PNR (μV)	M-wave (μV)	
				Frog				
Control	246 ± 23	246	45 ± 6	17.0	484 ± 57	451 ± 36	407 ± 48	
Ba^{2+}	211 ± 25	211	5 ± 2	2.6	521 ± 71	386 ± 33	96 ± 23	
	86%	86%	11%	15%	108%	86%	24%	
	(n = 14)		(n = 11)		(n = 14)	(n = 13)	(n = 13)	
				Salamander				
Control	201 ± 26		34 ± 5		346 ± 49	378 ± 29	381 ± 25	92 ± 19
Ba^{2+}	213 ± 23		2.8 ± 0.5		495 ± 55	315 ± 28	111 ± 19	19.8 ± 3.2
	106%		8%		143%	83%	29%	22%
	(n = 8)		(n = 4)		(n = 8)	(n = 8)	(n = 8)	(n = 17)

current flow through Müller cells and demonstrates that spatial buffering by glial cells in situ occurs during the course of normal neuronal activity. Glial cells may function in a similar fashion to regulate $[K^+]_o$ throughout the brain.

REFERENCES AND NOTES

1. R. K. Orkand, J. G. Nicholls, S. W. Kuffler, *J. Neurophysiol.* **29**, 788 (1966).
2. B. R. Ransom and W. G. Carlini, *Astrocytes*, S. Fedoroff and A. Vernadakis, Eds. (Academic Press, Orlando, 1986), vol. 2, p. 1.
3. A. R. Gardner-Medwin and C. Nicholson, *J. Physiol. (London)* **335**, 375 (1983); I. Dietzel, U. Heinemann, G. Hofmeier, H. D. Lux, *Exp. Brain Res.* **40**, 432 (1980); A. R. Gardner-Medwin, J. A. Coles, M. Tsacopoulos, *Brain Res.* **209**, 452 (1981); J. A. Coles and R. K. Orkand, *J. Physiol. (London)* **340**, 157 (1983).
4. C. J. Karwoski, *Physiol. Bohemoslov.* **37**, 217 (1988).
5. E. A. Newman, D. A. Frambach, L. L. Odette, *Science* **225**, 1174 (1984).
6. E. A. Newman, *J. Neurosci.* **5**, 2225 (1985).
7. S. S. Miller and R. H. Steinberg, *J. Membr. Biol.* **36**, 337 (1977).
8. C. J. Karwoski, D. A. Frambach, L. M. Proenza, *J. Neurophysiol.* **54**, 1607 (1985).
9. W. Walz, M. Shargool, L. Hertz, *Neuroscience* **13**, 945 (1984).
10. B. Rudy, *ibid.* **25**, 729 (1988).
11. M. L. Astion, J. A. Coles, R. K. Orkand, *Neurosci. Lett.* **76**, 47 (1987).
12. D. S. Henshel, P. L. Carras, P. A. Coleman, R. F. Miller, *Invest. Ophthalmol. Vis. Sci.* **26**, 116 (1985); E. A. Newman, *Nature* **317**, 809 (1985).
13. E. A. Newman, *J. Neurosci.* **7**, 2423 (1987).
14. J. D. Conner, P. B. Detwiler, P. V. Sarthy, *J. Physiol. (London)* **362**, 79 (1985).
15. C. J. Karwoski and L. M. Proenza, *J. Gen. Physiol.* **75**, 141 (1980).
16. ———, *J. Neurophysiol.* **40**, 244 (1977).
17. L. L. Odette and E. A. Newman, *Glia* **1**, 198 (1988).
18. Values of $[K^+]_o$ were calculated within the IPL (15 μm from the ganglion cell–IPL border) and 20 μm into the vitreous humor. Values of retinal layer thickness, extracellular volume fraction (α), and Müller cell conductance (g_{glia}) used in the simulation were as follows. [Format: retinal layer name, layer width (μm), α, g_{glia} (S cm^{-3})]: vitreous humor, 2750, 1.0, no glial cell; inner limiting membrane–endfoot, 2.5, 1.0, 330; nerve fiber layer, 17.5, 0.041, 6.72; ganglion cell layer, 25, 0.041, 0.504; IPL, 50, 0.182, 0.286; inner nuclear layer, 35, 0.048, 0.196; outer plexiform layer, 10, 0.182, 0.84; outer nuclear layer, 17.5, 0.048, 0.196; rod inner segment layer, 12.5, 0.198, 0.196; subretinal space, 60, 0.198, no glial cell; retinal pigment epithelium, 10, 0.0007, no glial cell. Volume fractions from (*8*), Müller cell conductance values from (*6*). Extracellular tortuosity factor, λ, 2.02; passive-uptake space volume fraction, 0.8; passive-uptake rate constant, 0.15 s^{-1}; active-uptake rate constant, 0.05 s^{-1}.
19. The simulated control K^+ response in the vitreous humor, although similar to the experimental response in time course, was smaller in amplitude (7% of the IPL response compared to 18% in experimental records; frog eyecups, diffuse flashes). This discrepancy may arise because we underestimated Müller cell K^+ conductance in the model or because we omitted (for simplicity) a light-evoked K^+ source in the ganglion cell layer.
20. C. J. Karwoski and E. A. Newman, *Vision Res.* **28**, 1095 (1988).

21. We thank B. Oakley II for suggesting the use of Ba^{2+} to test Müller cell function and L. L. Odette for assistance with the computer simulations. Supported by NIH grant EY 03526 to C.J.K. and grant EY 04077 to E.A.N.

13 January 1989; accepted 23 March 1989

Diffusible Factors Essential for Epidermal Cell Redifferentiation in *Catharanthus roseus*

BRUCE A. SIEGEL AND JUDITH A. VERBEKE*

During postgenital tissue fusions, some plant epidermal cells redifferentiate into parenchyma, a different cell type. Diffusible factors cause this response in the fusing gynoecium of the Madagascar periwinkle (*Catharanthus roseus*). Surgical manipulations of the gynoecium showed that epidermal cells from normally nonfusing surfaces could transmit and respond to the diffusible factors. Furthermore, the diffusible factors could be trapped in agar-impregnated barriers, as shown by the redifferentiation of carpel epidermal cells from nonfusing regions when the factor-loaded barriers were appressed to them.

EARLY IN ONTOGENY, CELLS AND TISSUES of common lineage diverge into contrasting paths of development as they respond to developmental signals (*1, 2*). This ability to develop in response to a specific signal is known as cellular competence (*3–6*) or cellular potentiality (*7*). As competent cells become committed to particular paths of differentiation, they are not readily diverted into other pathways; this restriction of the developmental potentiality of cells is referred to as determination (*8*).

In the absence of wounding (and usually in spite of wounding), virtually all plant epidermal cells are developmentally incompetent to redifferentiate (*9, 10*). This stable, differentiated state arises early in epidermal ontogeny (*11*). However, epidermal cells that take part in postgenital tissue fusions (*12*) are naturally occurring exceptions to this rule. These cells can redifferentiate. The postgenital tissue union that occurs in developing flowers of *Catharanthus roseus* L. (Apocynaceae) involves redifferentiation of epidermal cells in the young carpels, the structures in angiosperms that enclose the ovules

Department of Biological Sciences, University of Illinois at Chicago, Chicago, IL 60680.

*To whom correspondence should be addressed.

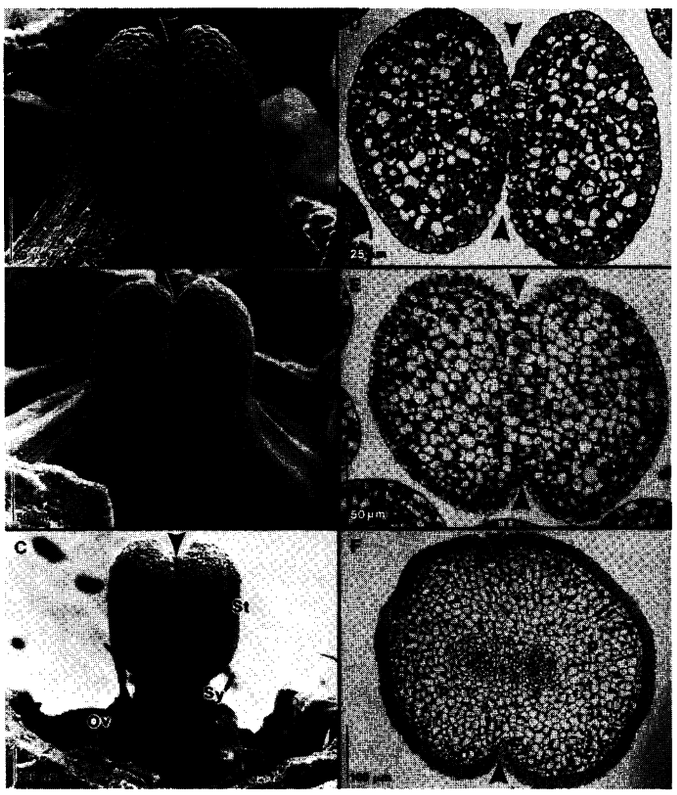

Fig. 1. Prefusion, fusing, and postfusion stages in *C. roseus* carpels. The large arrowheads indicate the plane of fusion. All tissue was fixed in 2% glutaraldehyde, postfixed in osmium tetroxide, and dehydrated in graded ethanol concentrations. Specimens for scanning electron microscopy (A to C) were dried to the critical point and gold-coated before observation. Light microscopy specimens (D to F) were embedded in Spurr's (*20*) epoxy resin; sections 0.90 μm thick were stained with 1% toluidine blue O. (**A**) Two prefusion carpels arise as separate primordia and grow toward each other until (**B**) the adaxial surfaces come into contact. (**C**) Cells in the fused region enlarge and develop into the stigma, style, and distal region of the ovaries. (**D**) Two separate carpels, each with an epidermal layer surrounding parenchyma. (**E**) As the adaxial surfaces of the carpels touch, epidermal redifferentiation (*13*) can be observed in some of the cells (open arrowheads). (**F**) All contacting adaxial epidermal cells subsequently redifferentiate and the carpels fuse. Abbreviations: St, stigma; Sy, style; Ov, ovaries; E, epidermal cells; and p, parenchyma.